The onset of Darcy-Bénard convection in an inclined layer heated from below

D. A. S. Rees, Bath, U.K., and A. P. Bassom, Sydney, Australia

Summary. We present an account of the linear instability of Darcy-Boussinesq convection in a uniform, unstably stratified porous layer at arbitrary inclinations α from the horizontal. A full numerical solution of the linearized disturbance equations is given and the detailed graphical results used to motivate various asymptotic analyses. A careful study shows that at large Rayleigh numbers two-dimensional instability can only arise when $\alpha \le 31.30°$. However it is also demonstrated that the maximum inclination below which this instability may be possible is the slightly greater value of $31.49°$ which corresponds to a critical Rayleigh number of 104.30.

1 Introduction

Natural convection in porous layers heated from below has been studied extensively since the pioneering works of Horton and Rogers [1], and Lapwood [2]. The horizontal layer, studied in detail by Lapwood, forms one the simplest problems of linearized stability theory in fluid mechanics. When the layer is of infinite horizontal extent the linearized equations yield roll solutions of any phase and orientation, and more complicated patterns may be expressed simply in terms of sums of suitable roll solutions (e.g., rectangular and hexagonal patterns) or integrals of roll solutions (e.g., the axisymmetric roll pattern described in terms of the zeroth-order Bessel function, J_0). The realized roll pattern then depends on the precise form of the initial disturbances and their subsequent nonlinear interactions. A weakly nonlinear analysis of rolls was presented by Palm, Weber and Kvernvold [3], and the nonlinear stability properties of these rolls may be gleaned from the papers by Rees and Riley [4], [5].

Some of this degeneracy in the instability mode is removed when the layer is inclined, for then the first instability to occur as the Rayleigh number increases takes the form of longitudinal rolls (Weber [6]). Experimental work by Bories, Combarnous and Jaffrenous [7], Bories and Combarnous [8], and Hollard et al. [9] shows that this simple theoretical scenario is actually more complicated in practice. For instance, polyhedral cells tend to arise when the inclination from the horizontal is less than about 15°. The existence and stability of polyhedral cells may be caused by nonlinear effects (e.g., the temperature dependence of viscosity) according to Weber [6], or perhaps by spatial restrictions imposed by having a finite layer in experiments. However, these practical results are yet to be fully explained.

Numerous other papers exist on this topic; see for example Bories and Monferran [10], Walch and Dulieu [11], and Caltagirone and Bories [12], [13] for further numerical solutions. Studies into the effect of incorporating Brinkman's extension to the ubiquitous Darcy law (see Nield and Bejan [14]) have been conducted by Vasseur, Wang and Sen [15] while Stores-

letten and Tveitereid [16] were concerned with the effect of material anisotropy. Work by
Lewis, Rees and Bassom [17] has quantified and confirmed Gill's [18] classic result that con-
vection in a vertical layer is stable, although another paper by Kwok and Chen [19] shows
that the inclusion of the Brinkman terms is sufficient to allow destabilisation at sufficiently
high Rayleigh numbers. Notwithstanding the substantial literature on this topic (the reader is
referred to text [14] for comprehensive details) there remain some unresolved questions
regarding the seemingly straightforward linearized stability problem for Darcy flow in an
inclined layer. Although longitudinal rolls are theoretically the most dangerous disturbance,
this is true only in certain circumstances, such as when the layer is of infinite spanwise extent.
When insulating sidewalls are present there are consequent restrictions on the wavelength of
the longitudinal roll, and the preferred pattern may then take the form of pairs of oblique
rolls (pairs are required to satisfy the sidewall boundary conditions, and the resulting plan-
form is rectangular), or two-dimensional transverse rolls. Apart from a few results at low
inclinations and an estimate for the maximum angle for which transverse rolls are unstable,
very little has been presented in the open literature on this aspect.

The primary objective of this present work is to provide an account of the linear stability
properties for Darcy flow in an inclined layer and thereby to address some of the outstanding
issues mentioned above. Of importance for our work is the observation that solutions of the
linearized equations for general roll orientations may be reduced to a corresponding trans-
verse roll solution which means that it is sufficient to restrict attention to two-dimensional
solutions. Below we present a comprehensive set of neutral stability curves and show that the
estimate forwarded by Caltagirone and Bories [13] that two-dimensional disturbances are line-
arly unstable for $\alpha < 31.8°$ is slightly too large. The neutral stability curves display distinctive
behaviors in the large wave number, small inclination angle limit as well in the $O(1)$ wave
number, large Rayleigh number case. Asymptotic analyses of these limits are undertaken, and
very good agreement with the numerical results is obtained.

The remainder of this work is laid out as follows. In the coming section we formulate the
governing equations for the problem of Darcy flow in an inclined porous layer and conduct
the stability analysis in Sect. 3. Here numerical calculations are used to delimit the fairly com-
plex geometry of the neutral curves, and the various asymptotic limits of these are addressed.
The paper closes with a short discussion.

2 Formulation

Consider the problem of free convection in an infinite layer of a saturated porous medium
bounded by two impermeable surfaces a distance d apart and inclined at an angle α to the
horizontal. The temperatures of the upper and lower surfaces bounding the medium are taken
to be uniform and equal to T_c and T_h, respectively, with $T_h > T_c$. Cartesian co-ordinates
$(\bar{x}, \bar{y}, \bar{z})$ are oriented such that the $\bar{y}$-axis is normal to the bounding surfaces of the layer, $\bar{x}$ is
aligned up the layer, and $\bar{z}$ is the spanwise coordinate which is horizontal. The fluid is
assumed to be such that Darcy's law holds and the Oberbeck-Boussinesq approximation is
valid. Further, the fluid and the isotropic porous matrix are taken to be in a state of thermal
equilibrium, and it is assumed that there is no influence of either inertia and boundary effects
as would be the case if either Forchheimer or Brinkman type terms (Nield and Bejan [14])
were present. The governing dimensional equations are then

$$\bar{u}_{\bar{x}} + \bar{v}_{\bar{y}} + \bar{w}_{\bar{z}} = 0\,, \qquad\qquad\qquad\qquad\qquad\qquad (2.1.1)$$

$$(\bar{u}, \bar{v}, \bar{w}) = -\frac{K}{\mu}\left(\bar{p}_{\bar{x}}, \bar{p}_{\bar{y}}, \bar{p}_{\bar{z}}\right) + \frac{\varrho g \beta K(T - T_c)}{\mu}\left(\sin\alpha, \cos\alpha, 0\right), \qquad (2.1.2-4)$$

$$\sigma T_{\bar{t}} + \bar{u}T_{\bar{x}} + \bar{v}T_{\bar{y}} + \bar{w}T_{\bar{z}} = \varkappa(T_{\bar{x}\bar{x}} + T_{\bar{y}\bar{y}} + T_{\bar{z}\bar{z}}), \qquad (2.1.5)$$

where $\bar{u}, \bar{v}$ and $\bar{w}$ denote the fluid flux velocities in the $\bar{x}, \bar{y}$ and $\bar{z}$ directions, respectively, $\bar{t}$ is the time, $\bar{p}$ the pressure and T the temperature. Further, ϱ denotes the density of the saturating fluid at $T = T_c, \mu$ its (assumed constant) viscosity and β the coefficient of cubical expansion. The permeability and thermal diffusivity of the saturated medium are taken to be K and $\varkappa$, respectively, and σ is the ratio of the heat capacity of the saturated porous medium to that of the saturating fluid. Lastly, g denotes gravity.

In this paper we shall concentrate exclusively on the two-dimensional onset problem and therefore will set $\bar{w} = 0$ and require all $\bar{z}$-derivatives to vanish. The rationale behind this restriction lies in the following observations: first we note that the presence of sidewalls placed at $\bar{z} = $ constant has no effect on a two-dimensional flow in a porous medium in which boundary effects are absent. Secondly, suitably located sidewalls will enable two-dimensional or oblique modes to be realisable in practice as more dangerous three-dimensional longitudinal vortices will be inhibited. Thirdly, it is possible to use a simple transformation along the lines of that used in Squire's theorem to show that disturbances aligned at an oblique angle may be reduced mathematically to an equivalent two-dimensional disturbance at a different wave number, Rayleigh number and angle of inclination; details of this transformation are given in the Appendix. The upshot of these properties is that the analysis of this paper forms the basis for a complete linearized theory and is not just a specific simplified case. Finally, we remark that the two-dimensional porous medium equations, when nondimensionalized, are identical to those governing convection in a suitably inclined Hele-Shaw cell. Thus the problem tackled here has practical relevance in two areas and is not merely an abstract mathematical exercise.

The variables are nondimensionalized by setting

$$(u, v) = \frac{d}{\varkappa}(\bar{u}, \bar{v}), \quad (x, y) = d^{-1}(\bar{x}, \bar{y}), \quad p = \frac{K}{\varkappa\mu}\bar{p}, \quad t = \frac{\varkappa}{d^2\sigma}\bar{t}, \quad \theta = \frac{T - T_c}{T_h - T_c}, \qquad (2.2)$$

so that Eqs. (2.1) reduce to

$$u_x + v_y = 0, \qquad (2.3.1)$$

$$u = -p_x + R\theta\sin\alpha, \qquad (2.3.2)$$

$$v = -p_y + R\theta\cos\alpha, \qquad (2.3.3)$$

$$\theta_t + u\theta_x + v\theta_y = \theta_{xx} + \theta_{yy}, \qquad (2.3.4)$$

in which the Darcy-Rayleigh number is defined as

$$R = \frac{\varrho g \beta K d(T_h - T_c)}{\mu\varkappa}. \qquad (2.4)$$

The introduction of the streamfunction, ψ, according to

$$u = -\psi_y, \qquad v = \psi_x, \qquad (2.5)$$

simplifies the equations further, and what remains is the coupled system

$$\psi_{xx} + \psi_{yy} = R(\theta_x\cos\alpha - \theta_y\sin\alpha), \qquad (2.6.1)$$

$$\theta_{xx} + \theta_{yy} = \psi_x\theta_y - \psi_y\theta_x + \theta_t, \qquad (2.6.2)$$

which has to be solved subject to the boundary conditions that $\psi = 0$ on both $y = 0$ and $y = 1$, and $\theta = 1$ on $y = 0$ and $\theta = 0$ on $y = 1$. In the following section we consider the onset of convection in detail.

3 Stability analysis

3.1 Analysis and numerical results

The basic flow solution corresponding to Eqs. (2.6) is given by

$$\psi = \psi_b \equiv -\frac{1}{2}\, y(1-y)\, R\sin\alpha\,, \qquad \theta = \theta_b \equiv 1-y \tag{3.1}$$

and is valid for all values of R and α. If this solution is subtracted from the full system (2.6) by setting $\psi = \psi_b + \psi_p$, $\theta = \theta_b + \theta_p$ and the resulting equations linearized we obtain

$$\nabla^2 \psi = R[\theta_x \cos\alpha - \theta_y \sin\alpha]\,, \tag{3.2}$$

$$\theta_t = \nabla^2 \theta + \psi_x + (R\sin\alpha)\left(y - \frac{1}{2}\right)\theta_x\,. \tag{3.3}$$

Here the 'p' subscript, which denotes the perturbation, has been omitted for the clarity of presentation, and ∇^2 is the usual two-dimensional Laplacian in the $x - y$ space.

The linear stability of the basic state (3.1) is determined by setting

$$\psi = \mathrm{i}f(y)\,\exp\{\mathrm{i}kx + \lambda t\}\,, \qquad \theta = g(y)\,\exp\{\mathrm{i}kx + \lambda t\}\,, \tag{3.4}$$

where k is the wave number of the disturbance, and it is recalled that this two-dimensional ansatz is justifiable for the reason given in Sect. 2. Of course neutral modes arise whenever $\mathrm{Re}(\lambda) = 0$ and the functions f and g satisfy

$$f'' - k^2 f = (kR\,\cos\alpha)\, g + \mathrm{i}(R\,\sin\alpha)\, g'\,, \tag{3.5.1}$$

$$g'' - k^2 g = kf - \mathrm{i}kR\,\sin\alpha\left(y - \frac{1}{2}\right)g + \lambda g\,, \tag{3.5.2}$$

subject to the boundary conditions

$$f(0) = f(1) = g(0) = g(1) = 0 \tag{3.6}$$

and the (chosen) normalisation constraint

$$g'(0) = 1\,. \tag{3.7}$$

System $(3.5)-(3.7)$, which constitutes an eigenproblem for $\mathrm{Im}(\lambda)$ and R, cannot be solved analytically save for the choice $\alpha = 0$ although the possibility of analytical solutions at isolated points in the parameter space cannot be precluded. For various angles of inclination α neutral curves may be computed which delimit the relationship between R and k, and these curves were computed using a finite difference method coupled to a matrix eigenvalue solver. The system was solved on a uniform grid, and the corresponding vector of values of f and g at these nodes was determined by the following strategy. Equations (3.5.1) and (3.5.2) were approximated using a 2nd-order accurate central difference approximation, and therefore the continuous functions were replaced by a pair of vectors containing the values of f and g at the
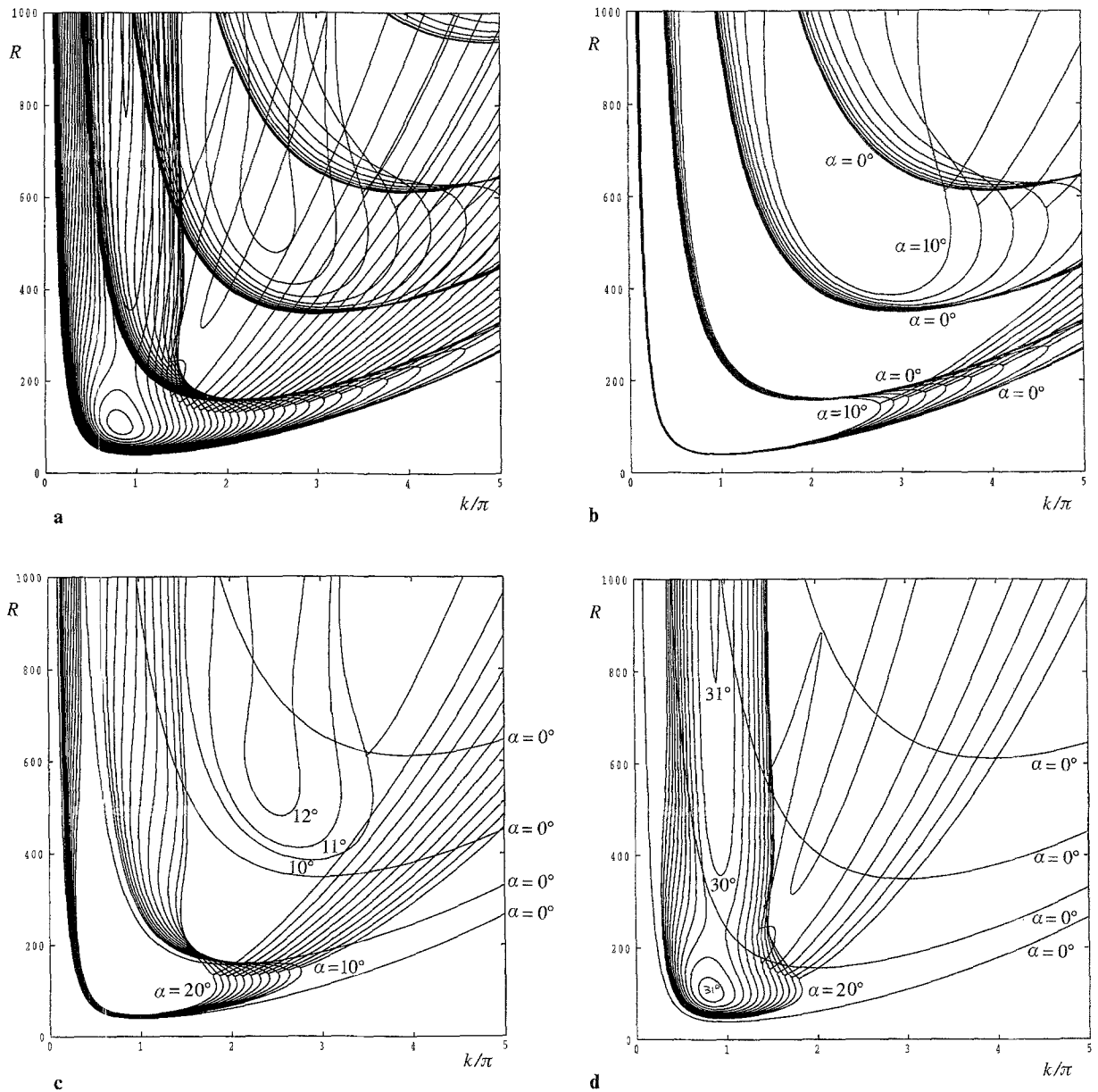
Fig. 1. Neutral curves corresponding to the first four modes of convection in an inclined layer. **a** The full set of curves for $0° \leq \alpha \leq 31°$ at intervals of $1°$; **b** Curves for $0° \leq \alpha \leq 10°$; **c** Curves for $10° \leq \alpha \leq 20°$; **d** Curves for $20° \leq \alpha \leq 31°$

grid points. Equation (3.5.1) was then used to find the vector of f-values in terms of the g-values, and this was done by inverting the tridiagonal system of equations which arises from the finite difference approximation. This vector was substituted into the discrete form of (3.5.2) which led to a matrix eigenvalue problem for λ and the g-vector. The eigenvalue problem was solved by use of the routine F02AJF taken from the NAG library, and some experimentation suggested that sufficiently accurate solutions for the range of values of R and k used in Fig. 1 could be determined by using about twenty points between $y = 0$ and $y = 1$. The eigenproblem (3.5)–(3.7) was solved on a rectangular grid in the $k - R$ parameter space

given by $0 \leq k \leq 5\pi$, $0 \leq R \leq 1000$ with a spacing of $\Delta k = \pi/50$ and $\Delta R = 2.5$ in the respective directions. Given these results a contour interpolation program was used to isolate the neutral curves for which $\mathrm{Re}(\lambda) = 0$, and it was found that this parameter domain is large enough so as to include the first four modes. This method, though formally less accurate than say a more straightforward fourth-order Runge-Kutta code with a multiple-shooting facility, yields the neutral curves very much more quickly. Moreover, a very significant advantage of the methodology adopted here is that disconnected solution branches cannot be overlooked, and therefore the results presented in Fig. 1 are guaranteed to be complete. The geometry of the neutral curves is quite complicated and, in order to aid interpretation, the full solutions for α up to about $31°$ shown in Fig. 1a are divided into approximately ten degree bands in Fig. 1b–d.

When $\alpha = 0$ Eqs. (3.5) can be solved analytically by setting both $f(y)$ and $g(y)$ proportional to $\sin n\pi y$, and the corresponding neutral curves, given by

$$R = \frac{(k^2 + n^2\pi^2)^2}{k^2}\,, \tag{3.8}$$

are clearly seen in Fig. 1: these neutral modes are stationary (i.e., $\mathrm{Im}(\lambda) = 0$) and the neutral curves $(n = 1, 2, \ldots)$ exist for all $k > 0$. There are a number of features of Fig. 1 that are deserving further attention, and these issues are tackled below. When $\alpha = 0$ the neutral curves corresponding to modes 1 and 2 (i.e., for $n = 1$ and $n = 2$ in (3.8)) are distinct from one another, as are those corresponding to modes 3 and 4, modes 5 and 6 and so on. When α is small we see that these respective pairs join together at a turning point where $dk/dR = 0$ at finite values of k. As an example of this phenomenon it is observed that for $\alpha = 3°$ this critical wavenumber is about 4.6: for smaller values of k there are the two stationary mode branches from which a travelling mode emerges and proceeds towards larger values of k. The point at which the travelling mode branch appears is not the turning point of the stationary mode curve, but is slightly above it; this is seen more clearly in Fig. 1c. As α increases to larger values the stationary mode neutral curves pinch off to form closed loops – these may be seen clearly in Fig. 1d for $\alpha = 30°$ and $31°$. At such inclinations there are no travelling mode curves, but an "open" loop remains at higher Rayleigh numbers. Eventually the closed loop disappears as α increases still further, and all computed values of $\mathrm{Re}(\lambda)$ on the $(R - k)$-grid are negative. A similar phenomenon occurs for modes 3 and 4, although the corresponding closed loops disappear at an angle just above $\alpha = 12°$.

3.2 Some specific neutral locations

We commence our study into the result of Fig. 1 by concentrating initially on the angle at which the stationary neutral modes cease to exist. If Fig. 1 is visualised as a two-dimensional projection of a three-dimensional surface, then the maximum value of α corresponds to where both

$$\frac{\partial\alpha}{\partial R} = 0 \qquad \text{and} \qquad \frac{\partial\alpha}{k} = 0\,. \tag{3.9}$$

If we denote $\hat{f} = \partial f/\partial R$ and $\tilde{f} = \partial f/\partial k$, with corresponding definitions for $\hat{g}$ and $\tilde{g}$, then separate differentiations of (3.5.1, 2) with respect to R and k, and the insistence that the formulae in (3.9) be satisfied yield the equations:

$$\hat{f}'' - k^2\hat{f} = (Rk\cos\alpha)\,\hat{g} + (iR\sin\alpha)\,\hat{g}' + (k\cos\alpha)\,g + (i\sin\alpha)\,g\,, \tag{3.10.1}$$

$$\hat{g}'' - k^2 \hat{g} = k\hat{f} - iRk \sin\alpha \left(y - \frac{1}{2} \right) \hat{g} - ik \sin\alpha \left(y - \frac{1}{2} \right) g + \lambda\hat{g} + \frac{\partial\lambda}{\partial R} , \tag{3.10.2}$$

$$\tilde{f}'' - k^2 \tilde{f} = (Rk \cos\alpha) \tilde{g} + (iR \sin\alpha) \tilde{g}' + 2kf + (R \cos\alpha) g , \tag{3.10.3}$$

$$\tilde{g}'' - k^2 \tilde{g} = k\tilde{f} - iRk \sin\alpha \left(y - \frac{1}{2} \right) \tilde{g} + \lambda\tilde{g} + 2kg + f - iR \sin\alpha \left(y - \frac{1}{2} \right) g + \frac{\partial\lambda}{\partial k} g . \tag{3.10.4}$$

As λ is purely imaginary at onset, $\partial\lambda/\partial R$ and $\partial\lambda/\partial k$ are also purely imaginary. The critical values for R, α and k are found by solving (3.5) and (3.10) subject to the boundary conditions (3.6), (3.7) and

$$\tilde{f} = \hat{f} = \tilde{g} = \hat{g} = 0 \quad \text{at} \quad y = 0, 1 \quad \text{and} \quad \tilde{f}' = \hat{f}' = 1 \quad \text{at} \quad y = 0 , \tag{3.11}$$

where the final two boundary conditions in (3.11) have be chosen as suitable normalising conditions. The system comprising (3.5) and (3.10) is not suited to solution using the matrix eigenvalue strategy, and therefore we resorted to a shooting method code founded upon Newton-Raphson iteration and a fourth-order Runge-Kutta scheme. This gave

$$R_c = 104.2959 , \qquad \alpha = 31.49032° \ (0.54961 \, \text{rad}) , \qquad k = 2.55532 = 0.81338\pi , \tag{3.12}$$

and also showed that $\text{Im}(\lambda) = \text{Im}(\partial\lambda/\partial R) = \text{Im}(\partial\lambda/\partial k) = 0$. The conclusion therefore is that this value of α represents the largest inclination of the layer for which linearized disturbances can grow.

The presence of a local maximum value of α is not restricted to solutions obtained from the first pair of modes. Figure 1 shows clearly that another occurs between the third and fourth modes. Use of the same code revealed that the critical parameter values are

$$R_c = 569.53 , \qquad \alpha = 12.29029° \ (0.21451 \, \text{rad}) , \qquad k = 7.75339 = 2.46798\pi , \tag{3.13}$$

and it is presumed that further maxima occur between higher modes, although we have not investigated this. Indeed, the precise evaluation of the results (3.13) proved to be very difficult principally because the large value of k yields a stiff system of equations. However use of Richardson extrapolation enabled the accuracy of the critical values to be improved and the values quoted in (3.12) to (3.14) are correct to the given number of decimal places.

One other position of interest is that just above the first local α-maximum and is the saddle point which marks the stage at which the single neutral curve pinches off and subdivides to form separate open and closed curves. The calculation of this point again presented severe numerical difficulties, but was found to be positioned at

$$R_c = 249.548 , \qquad \alpha = 29.234° \ (0.51024 \, \text{rad}) , \qquad k = 2.7743 = 0.8831\pi . \tag{3.14}$$

It is clear that predictions (3.12)–(3.14) are all consistent with the evidence provided in Fig. 1.

3.3 The large-k, small-α asymptotic analysis

We turn now to the behavior of the stationary mode curves at their turning points, that is, at those values of k for which $\partial k/\partial R = 0$, i.e. where the tangent to the neutral curve is vertical. Of particular interest is the behaviour of the turning point as $\alpha \to 0$ for we know that this must be a singular limit since the horizontal result (3.8) for $\alpha = 0$ holds for all k. We commence by investigating the behavior of the neutral curve when α is small but take k to be arbitrary.

The solution to Eq. (3.5) may be expanded as power series in α by introducing

$$(f, g, R, \lambda) =) f_0, g_0, R_0, \lambda_0) + \alpha(f_1, g_1, R_1, \lambda_1) + \alpha^2(f_2, g_2, R_2, \lambda_2) + \cdots, \tag{3.15}$$

and the resulting equations at the first three orders are

$$f_0'' - k^2 f_0 = R_0 k g_0, \tag{3.16.1}$$

$$g_0'' - k^2 g_0 = k f_0 + \lambda_0 g_0, \tag{3.16.2}$$

$$f_1'' - k^2 f_1 = R_0(k g_1 + i g_0') + R_1 k g_0, \tag{3.17.1}$$

$$g_1'' - k^2 g_1 = k f_1 - i R_0 k \left(y - \frac{1}{2} \right) g_0 + \lambda_0 g_1 + \lambda_1 g_0, \tag{3.17.2}$$

$$f_2'' - k^2 f_2 = R_0 \left(k g_2 + i g_1' - \frac{1}{2} k g_0 \right) + R_1(k g_1 + i g_0') + R_2 k g_0, \tag{3.18.1}$$

$$g_2'' - k^2 g_2 = k f_2 - i R_0 k \left(y - \frac{1}{2} \right) g_1 - i k R_1 \left(y - \frac{1}{2} \right) g_0 + \lambda_0 g_2 + \lambda_1 g_1 + \lambda_2 g_0, \tag{3.18.2}$$

subject to the boundary conditions that each f_n and g_n ($n = 0, 1, 2$) vanishes at both $y = 0$ and $y = 1$.

For the first mode the leading order problem yields

$$f_0 = -\frac{(\pi^2 + k^2)}{k} \sin \pi y, \qquad g_0 = \sin \pi y, \qquad R_0 = \frac{(\pi^2 + k^2)^2}{k^2}, \qquad \lambda_0 = 0, \tag{3.19}$$

where the normalization chosen is that the coefficient of $\sin \pi y$ in the definition of g_0 is unity. For neutrality $\text{Re}(\lambda_1) = 0$, and solutions of (3.17) can only be obtained if $R_1 = \text{Im}(\lambda_1) = 0$, whereupon

$$f_1 = \frac{(\pi^2 + k^2)^3}{8\pi k^2} i(y - y^2) \cos \pi y + \frac{(\pi^2 + k^2)^2 (k^2 + 5\pi^2)}{8\pi^2 k^2} i \left(y - \frac{1}{2} \right) \sin \pi y, \tag{3.20.1}$$

$$g_1 = -\frac{(\pi^2 + k^2)^2}{8\pi k} i(y - y^2) \cos \pi y - \frac{(\pi^2 + k^2)^2}{8\pi^2 k} i \left(y - \frac{1}{2} \right) \sin \pi y. \tag{3.20.2}$$

Given the above results, Eqs. (3.18) may be written in the simplified forms:

$$f_2'' - k^2 f_2 - R_0 k g_2 = R_0 \left(i g_1' - \frac{1}{2} k g_0 \right) + R_2 k g_0 \equiv \mathcal{R}_1, \tag{3.21.1}$$

$$g_2'' - k^2 g_2 - k f_2 = -i R_0 k \left(y - \frac{1}{2} \right) g_1 + \lambda_2 g_0 \equiv \mathcal{R}_2, \tag{3.21.2}$$

which define $\mathcal{R}_1$ and $\mathcal{R}_2$. Solutions to (3.21) subject to the appropriate boundary conditions can be obtained only if

$$\int_0^1 (\mathcal{R}_1 f_0 + \mathcal{R}_2 g_0 R_0) \, dy = 0, \tag{3.22}$$

and the satisfaction of this solvability condition requires

$$R_2 = \frac{(\pi^2 + k^2)^2}{32\pi^4 k^4} (\pi^6 + 23\pi^4 k^2 + 11\pi^2 k^4 + 5k^6) + \frac{(\pi^2 + k^2)^4 (\pi^2 - k^2)}{96\pi^2 k^4} + \frac{(\pi^2 + k^2) \lambda_2}{k^2}. \tag{3.23}$$

Setting $\lambda_2 = 0$ yields the $O(\alpha^2)$ correction to the critical value of the Rayleigh number in the absence of tilt, R_0. When $k = \pi$, the critical wave number for $\alpha = 0$, the corresponding

Rayleigh number reduces to

$$R_c = 4\pi^2 + 5\pi^2\alpha^2 + O(\alpha^3)\,, \tag{3.24}$$

which should be compared with $R_c = 4\pi^2/\cos\alpha = 4\pi^2 + 2\pi^2\alpha^2 + O(\alpha^4)$ which is the corresponding result for longitudinal rolls.

For the second mode we obtain all the above results from (3.19) onwards subject to the alteration that all appearances of π in the formulae are to be replaced by 2π. Indeed, the substitution of $n\pi$ in the place of π yields the corresponding result for the nth mode.

Turning to the question of the location of the turning point as $\alpha \to 0$ there is an obvious need to consider the limit $k \to \infty$. Given the definition of R in (3.15), R_0 in (3.19) and R_2 in (3.23) we obtain the following expressions in the limit of $k \gg 1$:

$$\text{Mode 1:} \qquad R \sim (k^2 + 2\pi^2 + \cdots) + \alpha^2\left(\frac{k^6(15-\pi^2)}{96\pi^4} + \cdots\right) + O(\alpha^4)\,; \tag{3.25.1}$$

$$\text{Mode 2:} \qquad R \sim (k^2 + 8\pi^2 + \cdots) + \alpha^2\left(\frac{k^6(15-\pi^2)}{1536\pi^4} + \cdots\right) + O(\alpha^4)\,. \tag{3.25.2}$$

These expressions indicate that the $O(\alpha^4)$ correction is positive for the first mode but negative for the second – qualitatively the same as depicted in Fig. 1. Clearly, if k is sufficiently large and, in particular, is as large as $O(\alpha^{-1/3})$ then the terms in (3.25) which are formally $O(\alpha^2)$ will be as large as the second term in the $O(1)$ expressions, and a rescaling is necessary. To pursue this requires the definitions

$$\alpha = \beta/k^3\,, \qquad R = k^2 S_0 + S_2 + \cdots\,, \qquad \lambda = \mathrm{i}\sigma + O(k^{-2})\,, \tag{3.26.1-3}$$

$$f = kF_0 + k^{-1}F_2 + \cdots\,, \qquad g = G_0 + k^{-2}G_2 + \cdots\,, \tag{3.26.4,5}$$

to be incorporated within (3.5). At leading order F_0 and G_0 satisfy

$$F_0 + S_0 G_0 = 0\,, \qquad F_0 + G_0 = 0\,, \tag{3.27.1,2}$$

from which all we can infer is that $S_0 = 1$. At next order

$$F_2 + G_2 = F_0'' - S_2 G_0\,, \qquad F_2 + G_2 = G_0'' + \mathrm{i}\beta\left(y - \frac{1}{2}\right)G_0\,, \tag{3.28.1,2}$$

which are consistent only if

$$F_0'' + \frac{1}{2}\left[\mathrm{i}\left(y - \frac{1}{2}\right)\beta - \mathrm{i}\sigma + S_2\right]F_0 = 0\,, \tag{3.29}$$

subject to $F_0(0) = F_0(1) = 0$. This complex valued Airy equation can be easily solved when $\beta = 0$ for then

$$F_0 \propto \sin n\pi y\,, \qquad S_2 = 2n^2\pi^2\,; \tag{3.30}$$

this form of F_0 recovers the shape of the leading order eigenfunction when $k = O(1)$ while S_2 yields the second term on the right hand sides of (3.25). The numerical solution of (3.29) for various values of β is shown in Fig. 2 where it may be seen that a pair of stationary modes ($\sigma = 0$) eventually coalesces into a pair of travelling waves (with $\sigma \neq 0$) as the scaled wave number β increases. For the first pair of modes this occurs when $S_2 \sim 57.00$ and $\beta \sim 196.997$; these values were obtained by solving simultaneously (3.29) and the equation obtained by differentiating (3.29) with respect to S_2 and setting $\partial\beta/\partial S_2 = 0$. Figure 3 shows the variation of R with k at the turning points obtained from both the numerical and asymptotic approaches, and it is clear that the agreement is excellent.
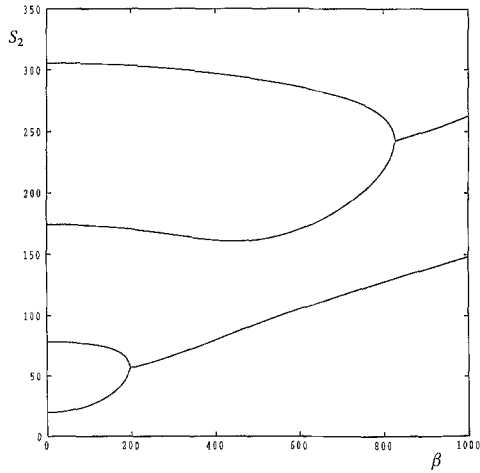
Fig. 2. Numerical solutions of eigenproblem (3.29) giving critical values of S_2 as a function of β
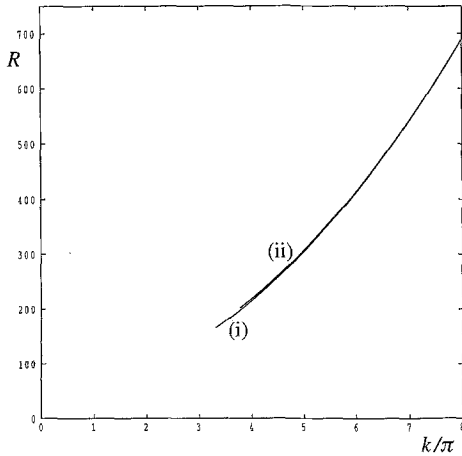
Fig. 3. A comparison between the values of R and k at the turning points in the curves obtained from (i) the fully numerical solution of system (3.5) and (ii) the asymptotic result $R \sim k^2 + 57.0 + \cdots$, $\alpha \sim 197/k^3 + \cdots$ valid for $k \gg 1$ (see text)

3.4 The large-R asymptotic analysis

Next we examine stationary mode solutions of the system (3.5) in the limit of large R and $\alpha, k = O(1)$. The symmetries of these equations when $\lambda = 0$ make it clear that solutions can be arranged so that $\mathrm{Re}(f)$ and $\mathrm{Re}(g)$ are functions which are even-valued about $y = 1/2$ while $\mathrm{Im}(f)$ and $\mathrm{Im}(g)$ are both odd about this point. In view of this, Eq. (3.5) was tackled asymptotically as $R \to \infty$ on $1/2 \leq y \leq 1$ subject to the impositions $\mathrm{Im}(f) = \mathrm{Im}(g) = 0$ on $y = 1/2$. Away from $y = 1/2$ it is anticipated that

$$f = \hat{f}_0 + \cdots , \qquad g = R^{-1}\hat{g}_0 + \cdots , \tag{3.31.1, 2}$$

and substitution into (3.5) gives that at leading orders

$$\hat{f}_0{}'' - k^2 \hat{f}_0 = (k \cos \alpha)\, \hat{g}_0 + (\mathrm{i} \sin \alpha)\, \hat{g}_0{}' , \tag{3.32.1}$$

$$\hat{f}_0 = \mathrm{i} \sin \alpha \left(y - \frac{1}{2} \right) \hat{g}_0 , \tag{3.32.2}$$

which combine to give

$$\left(y - \frac{1}{2}\right)(\hat{g}_0'' - k^2\hat{g}_0) + \hat{g}_0' + (ik\cot\alpha)\,\hat{g}_0 = 0\,. \tag{3.33}$$

It is an elementary exercise to develop series solutions of (3.33) valid for small values of $(y - (1/2))$, and linearly independent solutions exist, say $\phi_1(y)$ and $\phi_2(y)$, which have leading order behaviours $\phi_1 \sim \ln\left(y - (1/2)\right) + \cdots, \phi_2 \sim 1 + \cdots$ as $y \to 1/2$. By choice of normalisation we take

$$\hat{g}_0 = \phi_1(y) + \hat{\mu}\phi_2(y)\,, \tag{3.34}$$

where the choice of $\hat{\mu}$ is to be fixed. Our outer solution (3.31) is clearly of "inviscid" nature, and a thin layer surrounding $y = 1/2$ must be examined so as to ensure that the solution satisfies the necessary conditions on the symmetry line. This "boundary layer" is of depth $O(\varepsilon)$, where $\varepsilon^3 \equiv R^{-1}$, and if the $O(1)$ coordinate Y is defined according to

$$y = \frac{1}{2} + \varepsilon Y \tag{3.35.1}$$

then the eigensolutions must take the forms

$$f = \varepsilon\ln\varepsilon\hat{F}_0 + \varepsilon\hat{F}_1 + \cdots\,, \qquad g = \varepsilon^3\ln\varepsilon\hat{G}_0 + \varepsilon^3\hat{G}_1 + \cdots\,. \tag{3.35.2,3}$$

These functions satisfy

$$\frac{\mathrm{d}^2\hat{F}_j}{\mathrm{d}Y^2} = i\sin\alpha\,\frac{\mathrm{d}\hat{G}_j}{\mathrm{d}Y}\,, \qquad \frac{\mathrm{d}^2\hat{G}_j}{\mathrm{d}Y^2} = k\hat{F}_j - (ik\sin\alpha)\,Y\hat{G}_j\,, \tag{3.36.1,2}$$

for $j = 0, 1$.

Matching with the outer solution gives $\hat{G}_0 = 1$, $\hat{F}_0 = i\sin\alpha Y$ while $\hat{G}_1$ satisfies

$$\frac{\mathrm{d}^3\hat{G}_1}{\mathrm{d}Y^3} + (ik\sin\alpha)\,Y\,\frac{\mathrm{d}\hat{G}_1}{\mathrm{d}Y} = ik\sin\alpha\,, \tag{3.37}$$

subject to $\hat{G}_1 \to \ln(2kY) + \hat{\mu} + o(1)$ as $Y \to \infty$. The formal solution of (3.37) is

$$\hat{G}_1 = \gamma - \frac{\exp(-i\pi/3)}{3\mathrm{Ai}(0)\,\mathrm{Ai}'(0)}\left(\int_0^\zeta \mathrm{Ai}(t)\,\mathrm{d}t\right) - \int_0^\zeta \mathrm{Ai}(t)\left(\int_0^t \frac{\left[\int_\infty^q \mathrm{Ai}(s)\,\mathrm{d}s\right]}{\{\mathrm{Ai}(q)\}^2}\,\mathrm{d}q\right)\mathrm{d}t\,, \tag{3.38}$$

where $\zeta = (-ik\sin\alpha)^{1/3}\,Y$ and Ai denotes the usual Airy function. Our expectation that $\mathrm{Im}(f)$ and $\mathrm{Im}(g)$ should be odd-valued about $y = 1/2$ implies that the constant γ in (3.38) is real. Using well known properties of the Airy function, it follows that for (3.38) to have the correct behavior as $Y \to \infty$ then

$$\mathrm{Im}(\hat{\mu}) = -\frac{1}{2}\pi\,. \tag{3.39}$$

Given this condition we are now able to find the dependence of α on k for large R. Equation (3.33) was solved numerically subject to $\hat{g}_0 = 0$ at $y = 1$ and the behavior (3.34) as $y \to 1/2$ where $\hat{\mu}$ satisfies (3.39). The results are depicted in Fig. 4 where we compare the form of the neutral curves as predicted by the present asymptotic analysis with their form as found by numerical solution of the full governing system (3.5) with the Rayleigh number $R = 10^3$. The similarity is striking, and we note the significant prediction from the asymptotic work

a   b
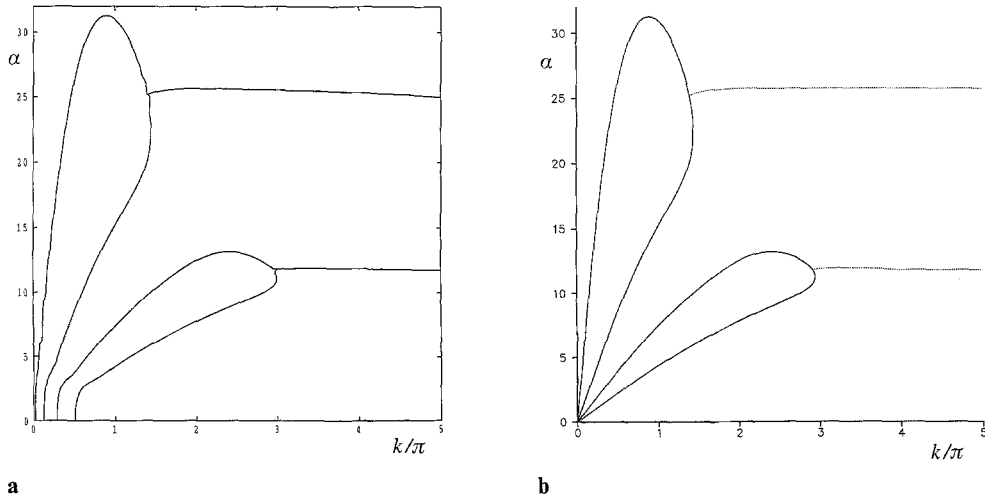
Fig. 4. A comparison between the neutral curves in the $\alpha-k$ space obtained from (**a**) the fully numerical solution of system (3.5) at $R = 10000$, and (**b**) the large-R asymptotic analysis derived using the numerical solution of (3.33) subject to (3.34) and (3.39)
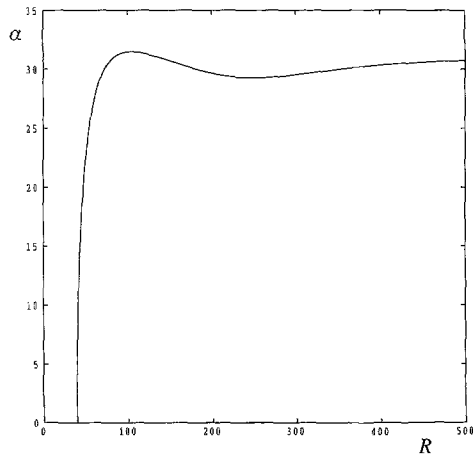
Fig. 5. The locus in the $\alpha-R$ parameter space of the maxima and minima (taken over the wave number k) of the curves of Fig. 1. At points above and to the left of the curve all perturbations of the form (3.4) are stable while below and to the right are the regimes in which some bands of wave numbers are unstable

that as $R \to \infty$ no neutral disturbances are possible for α greater than approximately $31.30°$. Note that although the comparison of the asymptotic and full numerical findings is very good for most values of α, the discrepancy in the results increases as $\alpha \to 0$. The reason for this can be traced to the fact that the asymptotic analysis outlined above holds good for $\alpha = O(1)$. Once α becomes small the analysis needs some modification: that this is so is easily seen from the exact result (3.8) valid for $\alpha = 0$; we can see that for prescribed R we can deduce a family of values of $k \neq 0$ for neutral modes. Thus the asymptotes on Fig. 4a cannot legitimately be extended all the way to $\alpha = 0$ for the assumptions underlying this derivation break down before then. Nevertheless, it is of considerable interest that the agreement between full numerical solutions and the corresponding asymptotic predictions is so good over a significant range of inclination angles.

It is concluded that the local maximum value of α given in Eq. (3.12.2) would seem to be the global maximum for the inclined layer, and this is confirmed by the results given in Fig. 5

where we plot the locus of the maxima and minima of the neutral curves over all wave numbers k. We remark on the global maximum at α as given by (3.12.2), a local minimum at the "pinch-off" point (3.14) and the large-R asymptotic value of $\alpha \approx 31.30°$.

4 Closing remarks

We have studied in detail the onset of convection in an inclined layer when the disturbances take the form of transverse rolls. As mentioned previously, these results are also applicable for oblique modes given a suitable transformation of the disturbance equations (see the Appendix) and are therefore of much wider use than might first appear. A numerical solution of the linear stability equations using a matrix eigenvalue solver based on discretised finite difference disturbance equations has shown that $\alpha = 31.490\,32°$ is the maximum inclination angle at which transverse modes can become unstable. This qualitative result is very different from that for an inclined fluid (as opposed to porous) layer for which transverse modes may be destabilised even in the vertical case $\alpha = \pi/2$. Given that Darcy-Brinkman flow in a vertical channel is also unstable, it would seem that the qualitatively different results arise because of the presence of diffusion terms in the momentum equations.

The detailed asymptotic analysis of turning points in the small-α, large-k limit gives very good agreement with the numerical results and shows that sufficiently large wave length disturbances must take the form of travelling modes. Further analysis has shown that when R is sufficiently large the practical limit on the inclination angle for instability is about $31.30°$. It is of some interest that the critical angle in the large Rayleigh number limit is marginally less than the overall maximum angle for instability.

Recent years have seen a much increased study of non-Darcy effects in general but this has not been greatly in evidence for porous layers. He and Georgiadis [20] showed that the presence of Forchheimer inertia terms does not affect the onset criterion for convection in a horizontal layer, but that the subsequent nonlinear development is changed: a result which was confirmed and quantified by some weakly nonlinear stability analysis given by Rees [21]. Further, when a mean horizontal pressure gradient is applied the induced flow serves to increase the critical Rayleigh number for the onset of convection in the presence of Forchheimer inertia (Rees [22]). But these three studies are concerned with horizontal layers. At present there are no papers which deal with either boundary or inertia effects with regard to their influence even on the linear stability of flow in an inclined layer. Thus an obvious next stage in the present line of study would be an adaptation so as to take these effects into account. The papers cited in the paragraph would suggest that such modifications to Darcy's law are very likely to play a significant role and thereby would modify the various stability criteria described herein.

Finally, it is necessary to point out that no conclusions may be drawn over whether strongly nonlinear convection exists at inclination angles greater than $\alpha = 31.490\,32°$. A thorough investigation of this would need to use weakly nonlinear theory to determine how finite-amplitude solution branches behave as $\alpha \to 31.490\,32°$. Further work might involve the corresponding large amplitude analysis using bifurcation continuation techniques, or the use of an energy stability analysis.

Appendix

In this appendix we derive the three-dimensional linearized stability equations and indicate how they may be reduced to an equivalent two-dimensional form. Beginning with the three-dimensional generalisation of system (2.3)

$$u_x + v_y + w_z = 0 \,, \tag{A1.1}$$

$$u = -p_x + R\theta \, \sin\alpha \,, \tag{A1.2}$$

$$v = -p_y + R\theta \, \cos\alpha \,, \tag{A1.3}$$

$$w = -p_z \,, \tag{A1.4}$$

$$\theta_t + u\theta_x + v\theta_y + w\theta_z = \theta_{xx} + \theta_{yy} + \theta_{zz} \,, \tag{A1.5}$$

the flux velocities may be eliminated to obtain the equivalent pressure/temperature formulation,

$$\nabla^2 p = R(\theta_x \, \sin\alpha + \theta_y \, \cos\alpha) \,, \tag{A2.1}$$

$$\nabla^2 \theta = R\theta(\theta_x \, \sin\alpha + \theta_y \, \cos\alpha) - p_x\theta_x - p_y\theta_y - p_z\theta_z + \theta_t \,, \tag{A2.2}$$

for which the basic solution is

$$p = p_b = R\left(y - \frac{1}{2}\,y^2\right)\cos\alpha + \frac{1}{2}\,Rx \, \sin\alpha \,, \qquad \theta = \theta_b = 1 - y \,, \tag{A3.1,2}$$

where the b-subscript denotes the basic flow and ∇^2 is three-dimensional Laplacian operator. Equations (A2) may be linearized about the basic solution to give

$$\nabla^2 p = R(\theta_x \, \sin\alpha + \theta_y \, \cos\alpha) \,, \tag{A4.1}$$

$$\nabla^2 \theta = R[(1-y)\,\theta_x \, \sin\alpha - \theta \, \cos\alpha] + p_y + \theta_t \,, \tag{A4.2}$$

for which solutions exist in the form:

$$p = f(y)\,\exp[\mathrm{i}k(x \, \cos\phi + z \, \sin\phi) + \lambda t] \,, \qquad \theta = g(y)\,\exp[\mathrm{i}k(x \, \cos\phi + z \, \sin\phi) + \lambda t] \,, \tag{A5}$$

where ϕ is the orientation of the roll away from that corresponding to the transverse roll. The functions f and g satisfy the equations

$$f'' - k^2 f = g(\mathrm{i}kR \, \cos\phi \, \sin\alpha) + g'(R \, \cos\alpha) \,, \tag{A6.1}$$

$$g'' - k^2 g = g[R\{\mathrm{i}k(1-y) \, \cos\phi \, \sin\alpha - \cos\alpha\} + \lambda] + f' \,, \tag{A6.2}$$

subject to the boundary conditions $f' = 0$ and $g = 0$ on both $y = 0$ and $y = 1$. Equations (A6) have four parameters, R, α, k and ϕ, but these may be reduced to three using the transformation

$$S = R\sqrt{\sin^2\alpha \, \cos^2\phi + \cos^2\alpha} \,, \qquad \tan\gamma = \tan\alpha \, \cos\phi \,, \tag{A7}$$

with which the equations reduce to

$$f'' - k^2 f = g[\mathrm{i}kS \, \sin\gamma] + g'[S \, \cos\gamma] \,, \tag{A8.1}$$

$$g'' - k^2 g = g[S\{\mathrm{i}k(1-y) \, \sin\gamma - \cos\gamma\} + \lambda] + f' \,, \tag{A8.2}$$

where the parameters are now S, γ and k. When $\phi = 0$ we have $S = R$ and $\gamma = \alpha$, and (A8) represents a set of disturbance equations with precisely the same solutions as Eqs. (3.5). When $\phi = \pi/2$ the disturbance takes the form of longitudinal rolls with $\gamma = 0$ and $S_c = 4\pi^2 = R/\cos\alpha$, as given by Weber [6]. When $\phi \neq 0$ with R, α and $k\cos\phi$ being set (the latter being the spanwise wave number of the disturbance; see (A5)) the corresponding values of S and γ are given by (A7), and the solution obtained is identical to that found by solving (3.5) with the values of R and α taken to be the current values of S and γ. Therefore every oblique mode is equivalent to a transverse mode.

References

[1] Horton, C. W., Rogers, F. T.: Convection currents in a porous medium. J. Appl. Phys. **16**, 367–370 (1945).

[2] Lapwood, E. R.: Convection of a fluid in a porous medium. Proc. Camb. Phil. Soc. **44**, 508–521 (1948).

[3] Palm, E., Weber, J. E., Kvernvold, O.: On steady convection in a porous medium. J. Fluid Mech. **54**, 153–161 (1972).

[4] Rees, D. A. S., Riley, D. S.: The effects of boundary imperfections on convection in a saturated porous layer: non-resonant wavelength excitation. Proc. Roy. Soc. Lond. A **421**, 303–339 (1989).

[5] Rees, D. A. S., Riley, D. S.: The effects of boundary imperfections on convection in a saturated porous layer: near-resonant wave length excitation. J. Fluid. Mech. **199**, 133–154 (1989).

[6] Weber, J. E.: Thermal convection in a tilted porous layer. Int. J. Heat Mass Transf. **18**, 474–475 (1975).

[7] Bories, S., Combarnous, M., Jaffrenous, J.-Y.: Observation des différentes formes d'écoulements thermoconvectifs dans une couche poreuse inclinée. Comptes Rendues Acad. Sci. Paris Ser. A **275**, 857–860 (1972).

[8] Bories, S., Combarnous, M.: Natural convection in a sloping porous layer. J. Fluid Mech. **57**, 63–79 (1973).

[9] Hollard, S., Layadi, M., Boisson, H., Bories, S.: Ecoulements stationnaires et instationnaires de convection naturelle en milieu poreux. Rev. Gen. Thermique **34**, 499–514 (1995).

[10] Bories, S., Monferran, L.: Condition de stabilité et échange thermique par convection naturelle dans une couche poreuse inclineé de grande extension. Comptes Rendues Acad. Sci. Paris Ser. B **274**, 4–7 (1972).

[11] Walch, J. P., Dulieu, B.: Convection naturelle dans une boite rectangulaire légèrement inclinée contenant un milieu poreux. Int. J. Heat Mass Transf. **22**, 1607–1612 (1979).

[12] Caltagirone, J. P., Bories, S. A.: Solutions numériques bidimensionnelles et tridimensionnelles de écoulement de convection naturelle dans une couche poreuse inclinée. Comptes Rendues Acad. Sci. Paris Ser. B. **190**, 197–200 (1980).

[13] Caltagirone, J. P., Bories, S. A.: Solutions and stability criteria of natural convective flow in an inclined porous layer. J. Fluid Mech. **155**, 267–287 (1985).

[14] Nield, D. A., Bejan, A.: Convection in porous media. Berlin: Springer 1992.

[15] Vasseur, P., Wang, C. H., Sen, M.: Natural convection in an inclined rectangular porous slot: the Brinkman-extended Darcy model. Trans. ASME J. Heat Transf. **112**, 507–511 (1990).

[16] Storesletten, L., Tveitereid, M.: Rayleigh-Bénard convection in an inclined porous layer with aniso-tropic permeability. Adger Distriktshøgskole Report No. **63**, 1993.

[17] Lewis, S., Bassom, A. P., Rees, D. A. S.: The stability of vertical thermal boundary layer flow in a porous medium. Europ. J. Mech. B: Fluids **14**, 395–408 (1995).

[18] Gill, A. E.: A proof that convection in a porous vertical slab is stable. J. Fluid Mech. **35**, 545–547 (1969).

[19] Kwok, L. P., Chen, C. F.: Stability of thermal convection in a vertical porous layer. Trans. ASME J. Heat Transf. **109,** 889–893 (1987).

[20] He, X. S., Georgiadis, J. G.: Natural convection in porous media: effect of weak dispersion on bifurcation. J. Fluid Mech. **216,** 285–298 (1990).

[21] Rees, D. A. S.: The effect of inertia on the stability of convection in a porous layer heated from below. J. Theor. Appl. Fluid Mech. **1,** 154–171 (1996).

[22] Rees, D. A. S.: The effect of inertia on the onset of mixed convection in a porous layer heated from below. Int. Comm. Heat & Mass Transf. **24,** 277–283 (1997).

Authors' addresses: Dr. D. A. S. Rees, Department of Mechanical Engineering, University of Bath, Claverton Down, Bath BA2 7AY, U.K.; Dr. A. P. Bassom, New College, Anzac Parade, University of New South Wales, Sydney 2052, Australia (Permanent address: School of Mathematical Sciences, University of Exeter, North Park Road, Exeter EX4 4QE, Devon, U.K.)